Molecular Crystals and Liquid Crystals

Publication details, including instructions for authors and subscription information:
http://www.tandfonline.com/loi/gmcl20

Hybrid Nematic Films: A Detailed Monte Carlo Investigation

C. Chiccoli [a], S. P. Gouripeddi [b], P. Pasini [a], K. P. N. Murthy [b], V. S. S. Sastry [b] & C. Zannoni [c]

[a] Istituto Nazionale di Fisica Nucleare, Sezione di Bologna, Via Irnerio, Bologna, Italy

[b] School of Physics, University of Hyderabad, Central University P.O., Hyderabad, India

[c] Dipartimento di Chimica Fisica e Inorganica and INSTM-CRIMSON, Università di Bologna, Viale Risorgimento, Bologna, Italy

Version of record first published: 18 Mar 2009

To cite this article: C. Chiccoli, S. P. Gouripeddi, P. Pasini, K. P. N. Murthy, V. S. S. Sastry & C. Zannoni (2009): Hybrid Nematic Films: A Detailed Monte Carlo Investigation, Molecular Crystals and Liquid Crystals, 500:1, 118-131

To link to this article: http://dx.doi.org/10.1080/15421400802714072

Mol. Cryst. Liq. Cryst., Vol. 500, pp. 118–131, 2009

ISSN: 1542-1406 print/1563-5287 online
DOI: 10.1080/15421400802714072

Taylor & Francis
Taylor & Francis Group

Hybrid Nematic Films: A Detailed Monte Carlo Investigation

C. Chiccoli[1], S. P. Gouripeddi[2], P. Pasini[1], K. P. N. Murthy[2], V. S. S. Sastry[2], and C. Zannoni[3]
[1]Istituto Nazionale di Fisica Nucleare, Sezione di Bologna, Via Irnerio, Bologna, Italy
[2]School of Physics, University of Hyderabad, Central University P.O., Hyderabad, India
[3]Dipartimento di Chimica Fisica e Inorganica and INSTM-CRIMSON, Università di Bologna, Viale Risorgimento, Bologna, Italy

We present detailed Monte Carlo (MC) simulations of a nematic film with antagonistic boundary conditions corresponding to homeotropic and homogeneous planar anchoring at the two surfaces. The simulations are based on the Lebwohl-Lasher lattice spin model with boundary conditions chosen to mimic the cell anchoring. We have investigated the model using both a standard Metropolis and a reweighting Monte Carlo method recently implemented for continuous systems.

Keywords: anchoring; hybrid films; Monte Carlo; nematic liquid crystals; Wang-Landau algorithm

INTRODUCTION

Confined nematics exhibit peculiar physical phenomena connected to fundamental liquid crystal (LC) properties and to various important applications [1,2]. The confining surfaces, for instance curved and/or

We acknowledge the Indo-Italian program of cooperation in Science & Technology 2005–2007, Area: Materials Science & Technology, promoted by the Italian and Indian Ministries for Foreign Affairs. C.Z. is grateful to MUR (PRIN *Cristalli Liquidi*), and INSTM, while C.C. and P.P. thank INFN (grant I.S. BO62) for support. All the computations were carried out at the Centre for Modelling Simulation and Design, University of Hyderabad. GSP would like to thank Department of Atomic Energy, India, for providing fellowship during the period of this work.

Address correspondence to Paolo Pasini, INFN, Sezione di Bologna, Via Irnerio 46, Bologna 40126, Italy. E-mail: Paolo.Pasini.@bo.infn.it

possibly with antagonistic boundary conditions, can result in competing multiple minima in free energy space, leading to frustration as well as to observable transitions between a variety of non-trivial equilibrium structures which would be otherwise difficult to realize [2]. The overall effect on the director field is difficult to predict, as in confined systems there is in general a competition between effects due to the boundary conditions, the ordering interactions inside the LC system, and the disordering effects due to the temperature [3]. Different organizations can be obtained as a function of some suitable external driving parameters changing the easy axis at the boundaries (e.g., by irradiation of azobenzene covered surfaces [4] or, more frequently, just by applying an external field or changing the temperature. A typical example of confinement leading to competing mechanisms [5,6] is that shown by hybrid nematic films [2,7–11], where a liquid crystal layer is placed between two plates, typically with lateral dimensions much greater than the thickness, and with antagonistic boundary conditions: homeotropic at $z = d$ to planar at $z = 0$. In this system two limiting structural organizations can exist. The first corresponds to a continuous deformation of the director across the sample between the two easy axis directions. The other is a "biaxial" or "director-exchange" configuration with uniaxial alignment close to each of the two substrates and a sudden switch from one to the other [7,8,11]. From continuum theory and Frank free energy minimization methods [7,8] these opposite boundary conditions are expected to cause, for sufficiently thin films, a structural transition from the bent-director to the biaxial structure. The biaxial structure should be formed only when the thickness of the liquid crystal film is below a certain critical value (estimated at $\sim$47 nm for the nematic 5CB [10,11]). On the other hand, at fixed thickness, a transition from a biaxial organization to a continuous variation of the director orientation across the cell is expected when the temperature of the system is lowered [8,10]. The system can be conveniently studied by computer simulations of a Lebwohl-Lasher type lattice model [3,12], that represent a powerful tool for studying ordering and structural transitions in uniaxial [13] and biaxial [14] nematics and their defects [3,5,10,15], particularly when the effect of complex boundaries and temperature has to be investigated. For instance, multiple organizations were also predicted and confirmed by Monte Carlo simulations [3,5] on a closely related system with degenerate, rather than uniform boundary condition, at the planar anchoring surface.

For the hybrid film, our previous canonical ensemble Monte Carlo simulations based on Lebwohl-Lasher lattice spin model [10] have confirmed that indeed two different structures can be formed.

Moreover, if the thickness allows the formation of the biaxial phase, two transitions occur as the temperature is varied. Upon cooling from the disordered isotropic phase, the first transition was clearly seen to be to the biaxial phase, and the second from the biaxial phase to a bent-director nematic phase.

Not surprisingly, given the complexity of the system, various points remain unclear, in particular concerning the extent of the physical region joining the two uniaxial nematic domains forming the biaxial phase and the effects of anchoring strengths.

To get a better understanding of this system here we wish to present a detailed investigation of the hybrid cell by using both the standard canonical Monte Carlo methods as well as [16], a multicanonical Monte Carlo method based on the Wang-Landau algorithm [17] recently applied to studying the nematic-isotropic phase transition [18].

We shall discuss, in particular, the effects of changing the anchoring strength, that was not investigated in [10], and the thickness of the hybrid nematic film.

THE SIMULATION MODEL

The Monte Carlo simulations were based on the simple and well studied Lebwohl-Lasher (LL) lattice spin model [12,13] already successfully employed in [10]. The particles interact through the attractive nearest neighbors LL pair potential

$$U_{i,j} = -\varepsilon_{ij} P_2(\boldsymbol{u_i} \cdot \boldsymbol{u_j}), \tag{1}$$

where

$$\varepsilon_{i,j} = \begin{cases} \varepsilon, & \varepsilon > 0 \textit{ for } i,j \textit{ nearest neighbours} \\ 0 & \textit{otherwise}, \end{cases} \tag{2}$$

$\boldsymbol{u_i}$, $\boldsymbol{u_j}$ are unit vectors along the axis of the two particles ("spins") and P_2 is a second rank Legendre polynomial. The spins represent a cluster of neighboring molecules whose short range order is assumed to be maintained through the temperature range examined [3]. The bulk Nematic-Isotropic (*NI*) transition for this model occurs at a reduced temperature $T^* \equiv \mathrm{kT}/\varepsilon = 1.1232$ [13].

The different boundary conditions are mimicked assuming a layer of outside particles with a fixed orientation consistent with the desired type of alignment at the top and at the bottom surfaces [3]. As we have mentioned before, in this work we need to consider hybrid boundary conditions which are homeotropic at the top surface while at the

bottom the alignment is considered to be always planar and homogeneous (along the x direction).

The anchoring strength at the top and bottom surfaces can be tuned by considering a different value of ε_{ij} when the spin j belongs to the additional layers. Periodic boundary conditions are instead employed at the four lateral surfaces of the simulated sample.

To generate the lattice configurations we have used the standard Metropolis Monte Carlo procedure [16] where one spin at a time is updated as described in [3] or a non-Boltzmann sampling using the Wang-Landau algorithm [17,18].

We schematically recall the basic idea of the relatively less well known Wang-Landau (WL) algorithm. If a random walk with a transition probability proportional to the reciprocal of a chosen function of energy, say *g(E)* is performed, the resulting probability distribution is given by

$$P(E) = \exp\left(\frac{S(E)}{k_B} - \ln[g(E)]\right), \tag{3}$$

where *S(E)* is the micro-canonical entropy and k_B is the Boltzmann constant. It is clear that if $S(E)/k_B = \ln[g(E)]$, then *P(E)* is same for all energy values E and the histogram of all the microstates so visited becomes flat. This maps to choosing *g(E)* corresponding to the density of states of the system, which however is not known a priori. Following the WL method the system is algorithmically guided through a learning process leading asymptotically to the estimate of the density of states. Thus, to start with we set all entries to $g(E_i) = 1$ for all i. Each time an energy level E_i is visited, we modify the density of states as

$$g(E_i) \to g(E_i)f_i \quad or \quad \ln[g(E_i)] \to \ln[g(E_i)] + \ln(f_i) \tag{4}$$

where the WL factor $\ln(f_i) \geq 1$. We use the updated density of states in the next step. In general, if x_1 and x_2 are two microstates before and after the local trial energy change in the configuration space, the move from x_1 to x_2 is accepted with the probability given by

$$p(x_1 \to x_2) = \min\left[\frac{g\{E(x_1)\}}{g\{E(x_2)\}}, 1\right] \tag{5}$$

Using this basic idea the WL algorithm was modified to study continuous systems [18] and an example of the density of states and of the ensemble is reported in Figure 1. All the desired physical observables are obtained by un-weighting with the density of states and

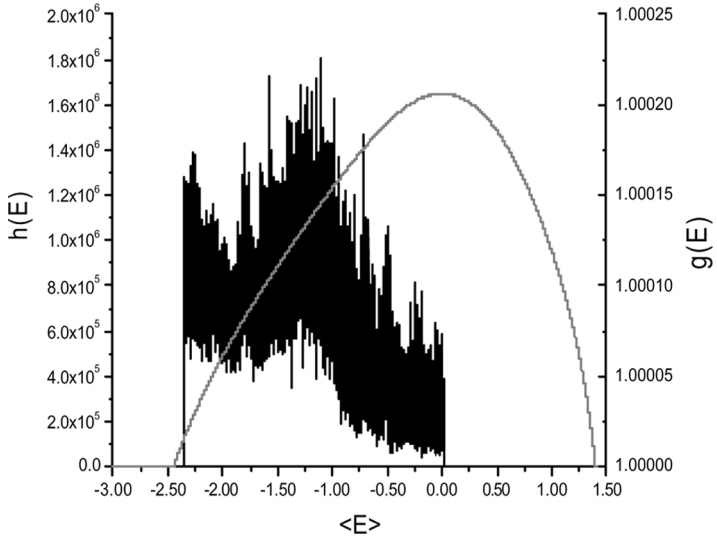

FIGURE 1 Density of states and the ensemble as obtained from the simulation of a $15 \times 15 \times 10$ hybrid system.

reweighting with the Boltzmann factor at the given temperature. The average of an arbitrary observable can be written as:

$$\langle O \rangle = \frac{\sum_{E_i} O(E_i) \exp(-\beta E_i + \alpha(E_i))}{\sum_i \exp(-\beta E_i + \alpha(E_i))} \tag{6}$$

with $\beta \equiv (1/\mathrm{kT})$ and $\alpha(E_i) = \ln[\mathrm{g}(E_i)]$.

SIMULATION RESULTS

Using first the standard Metropolis Monte Carlo method we have performed a set of independent complete simulations for a wide temperature range for some selected values of the film thickness d. The simulated films are $\mathrm{L} \times \mathrm{L} \times (d+2)$ lattices, with $\mathrm{L} = 15$, 30 and $d = 4$, 6, 8, 10, 12, 16, and 22. Using the WL multi-canonical algorithm we have further studied four systems of dimensions $15 \times 15 \times d$, where $d = 4$, 5, 6, and 10. The anchoring strength of the two substrates, ε_1 and ε_2 defined in units of LC-LC interaction (ε), was independently changed in steps of 0.25 from 0.25 to 1. During canonical sampling, the average of every quantity is taken over one million microstates for every temperature. The Wang-Landau runs were performed over

80 iterations, in order to get a well converged density of states. Based on this density, a production run was performed and about 5 million micro states were collected. Microstates uniformly distributed in energy (flat histogram of microstates along energy axis) along with the knowledge of the density of states can now be used to build canonical ensembles at any arbitrarily chosen temperature. Every state collected was un-weighted with the density of states and reweighted with the Boltzmann factor at this chosen temperature. All the observables were collected for every temperature, with a precision to the second decimal digit. More specifically, we calculate energy, $\langle \mathrm{E} \rangle$, specific heat ($C_v$), computed as the fluctuations in the energy of the system, the scalar second rank order parameter ($\mathrm{S} \equiv \langle \mathrm{P2} \rangle \lambda$), as obtained from the largest eigenvalue of the ordering matrix Q_{ij}, for the whole system and at each layer of the film [3,13], a biaxiality parameter (P) defined as:

$$P = |Q_{jj} - Q_{kk}|\sqrt{2}$$

where $jj, kk \neq ii$. We have also calculated the nematic order parameter $\langle P_2 \rangle_{\mathrm{z}}$ with respect to the z laboratory fixed direction:

$$\langle P_2 \rangle_z - \frac{3}{2N_L} \sum_{i=1}^{N_L} (u_i^{(L)} \cdot z)^z, \tag{7}$$

where $u_i^{(L)}$ is the direction of the ith spin belonging to layer L and N_L is the number of particles in that layer. In Figure 2 we report the variation of $\langle P_2 \rangle_{\mathrm{z}}$ across the cell for the various film thicknesses at four different temperatures. The dependence of the order at each layer on the thickness is noticeable, especially at the center of the cell, where the influence of the surfaces is the lowest. We see that for the thinner films ($d = 6,8$) the ordering changes regularly from being on average perpendicular ($\langle P_2 \rangle_{\mathrm{z}} < 0$) to parallel ($\langle P_2 \rangle_{\mathrm{z}} > 0$) to z at all temperatures, even above the bulk T_{NI}. In these cases we do not see a biaxial structure. However, for the thicker films: $d = 16$ and 22, the change of behavior with T^* is apparent. While for $T^* \leq 1.1$ the $\langle P_2 \rangle_{\mathrm{z}}$ is still regularly increasing, at $T^* = 1.2$ a plateau with $\langle P_2 \rangle_{\mathrm{z}}$ ~ 0 appears. The situation is less clear for the intermediate thickness corresponding to $d = 10$ and 12.

In Figure 3 we report the bending parameter $\mathrm{Q_{xz}}$ [10], which defines the coupling between the two preferred directions x and z and that should help to distinguish between the biaxial and bent-director structure [10]. We see that at the highest temperature $\mathrm{Q_{xz}} \sim 0$ in all cases, while fairly large values are shown up to $T^* = 1.1$ for thickness $d = 12$, 16, and 22.

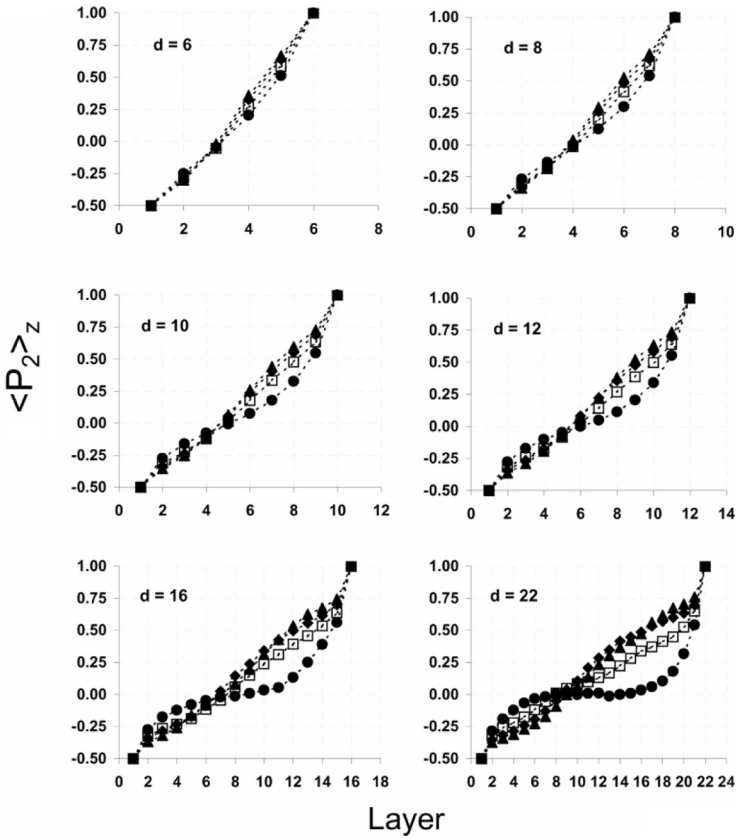

FIGURE 2 The second rank order parameter $\langle P_2 \rangle_z$, calculated at each layer of the hybrid cell, for various values of the film thickness d at $T^* = 0.9$ (▲), 1.0 (◆), 1.1 (□), and 1.2 (●). The lateral dimension of the system is $L = 30$.

To examine the nature of the change of organization we resort to the WL MC calculations, that allow a detailed study as a function of temperature. We report first results of WL Monte Carlo simulations for a sample of dimensions $15 \times 15 \times 10$ with the anchoring strength at every substrate set at $\epsilon_1 = \epsilon_2 = 1.00$ (i.e., LC-LC and LC-wall interaction strength have again the same value and the value is the same at both walls). We notice that the heat capacity C_V, obtained from the mean square fluctuations in the energy, shows a peak at a temperature $T_2^* = 1.183$ and a shoulder at $T_1^* = 1.09$ (Fig. 4, right scale). A tilt angle ϕ_i with respect to z-axis is also obtained diagonalizing the local Q tensor at each layer [10] and is plotted as a function of temperature

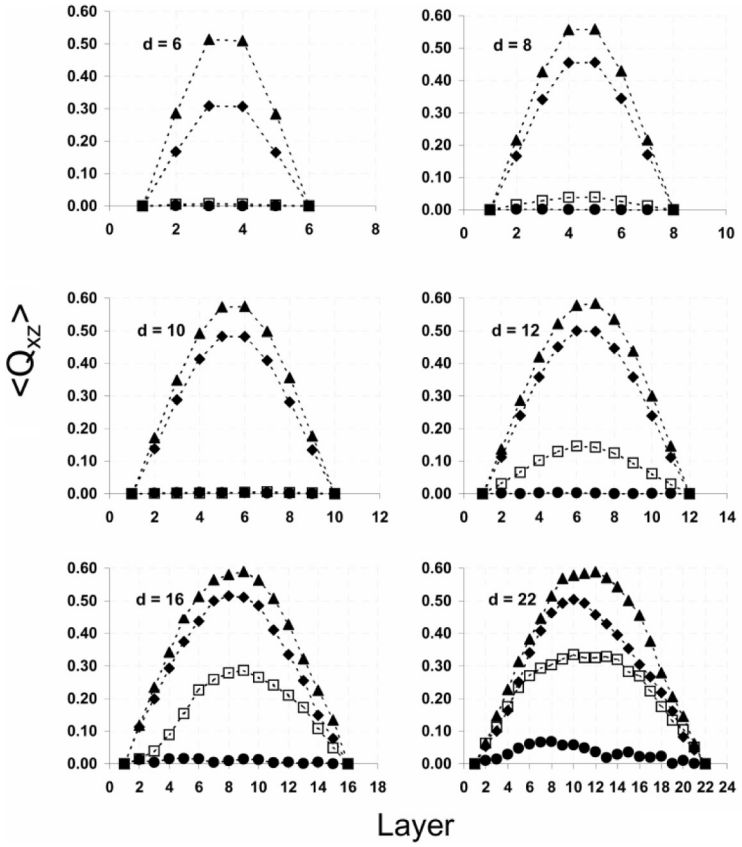

FIGURE 3 The bending parameter Q_{xz} at each layer of the hybrid cell, for various values of the film thickness d at $T^* = 0.9$ (▲), 1.0 (◆), 1.1 (□), and 1.2 (●). The lateral dimension of the system is $L = 30$.

in Figure 4. We see from the tilt angle (Fig. 4, left scale) that the transition at $T^* = 1.183$ corresponds to a transition from a disordered state to a biaxial-nematic phase, where the layers close to each surface assume a tilt consistent with their anchoring direction. The shoulder at $T^* = 1.09$ seem to indicate a structural transition, from biaxial-nematic phase to a bent-director nematic phase, as we can notice that deep in the nematic phase the angle ϕ_i uniformly decreases from 90° at the first layer of fixed spins to 0° at the other layer of fixed spins. The structure corresponds to the continuously changing director field in the bent-director structure. At temperatures above a certain threshold (about $T^* = 1.2$) the curves of the layers, progressively less affected

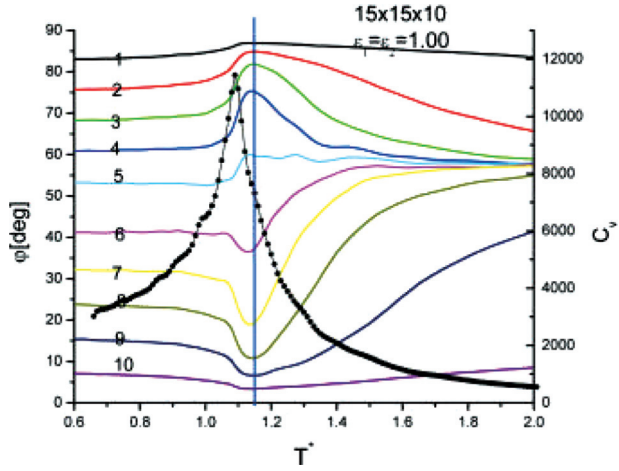

FIGURE 4 Director's tilt angle with respect to the z axis (left scale) and the fluctuations in energy (right scale) as a function of temperature. The angle is calculated at each distinct layer for a $15 \times 15 \times 10$ system and anchoring strengths $\varepsilon_1 = \varepsilon_2 = 1$. The results are obtained by a Non-Boltzmann (Monte Carlo) simulations and lines are guides to the eye.

by the substrates, approach a tilt angle value of 53°, which is close to the zero of the function P_2 (the so-called magic angle). However, since the director itself cannot be defined at higher temperatures in the absence of orientational order, the tilt angles depicted in the temperature region are only illustrations of the on-set of a disordered phase.

To investigate the effect of anchoring strength a system of dimension $15 \times 15 \times 6$ was then examined in detail, progressively reducing the coupling to the surfaces. The system was first studied by fixing the anchoring strength of both substrates at 1.00 ($\varepsilon_1 = \varepsilon_2 = 1.00$). It was found from C_V (not shown) that, similar to the system with 10 layers, two transitions occur. The transition from disordered phase to biaxial phase is at $T^* = 1.160 \pm 0.001$ and the other is at 1.050 ± 0.001. It was observed that the maximum peak of the biaxiality P corresponds to a temperature intermediate between the two transitions (Fig. 5, right).

The dependence of the biaxial order parameter on the temperature for the whole system and for each layer showed that on increasing the temperature we observe an increase of the biaxiality up to a transition to the isotropic state. This biaxiality increase is more pronounced in the center of the cell as can be seen by the data reported for the central layers (Fig. 6).

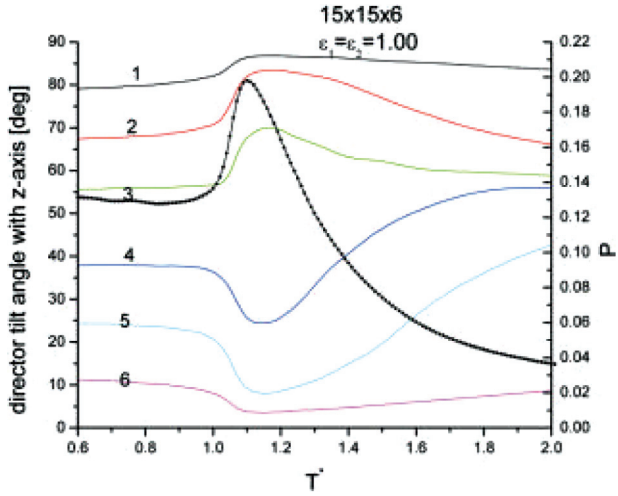

FIGURE 5 Variation of director tilt angle with z-axis and the biaxiality with temperature for a $15 \times 15 \times 6$ system ($\varepsilon_1 = \varepsilon_2$).

The anchoring strength of the substrates was then reduced in successive steps of 0.25 from 1 to 0 and all the properties were re-computed for each anchoring strength. It should be noticed that with the decrease in anchoring strength the signature of the higher temperature transition was not visible in the specific heat. On the

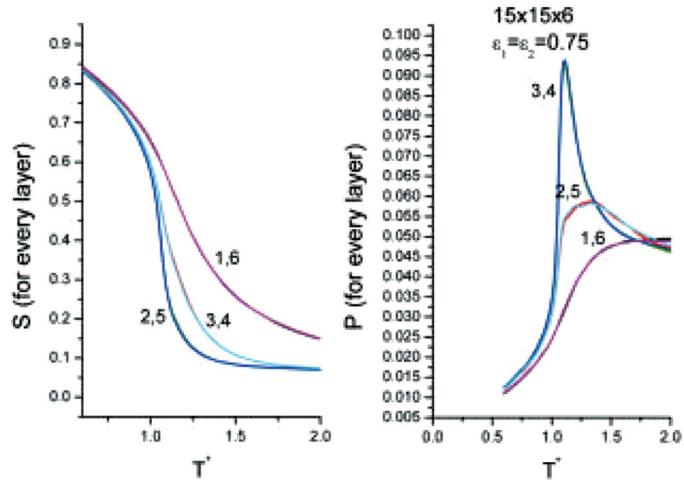

FIGURE 6 The layer-wise nematic (left) and biaxial (right) order parameters with change in temperature.

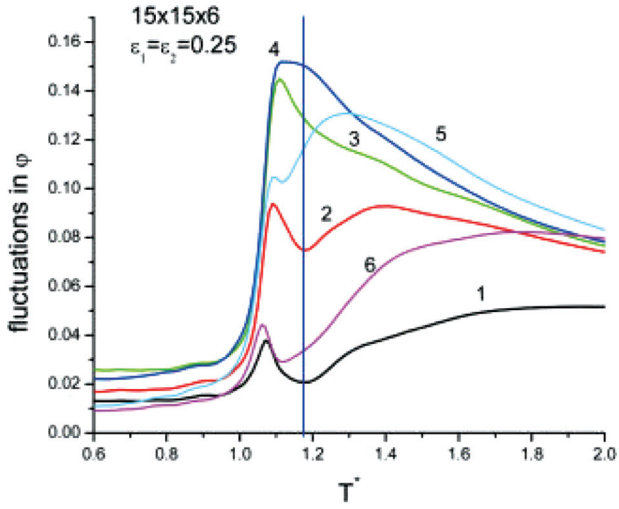

FIGURE 7 Fluctuation of the tilt angle with temperature for a $15 \times 15 \times 6$ system and $\varepsilon_1 = \varepsilon_2 = 0.25$.

other hand the fluctuations in the tilt angle gave a clear signature for this transition (Fig. 7) and this helped to find the transition temperature of the ordering transition for small anchoring strengths of the substrates. The transition becomes sharper with the decrease in anchoring strength. Correspondingly, the order is minimum and biaxiality maximum for maximum anchoring strength ($\varepsilon = 1.00$).

To get a better appreciation of the effect of the thickness of the liquid crystal films three systems were studied $15 \times 15 \times d$, where $d = 6$, 5, and 4. A bent structure was observed for systems of all the three thickness. In all the systems there were two transitions occurring first from disordered state to a biaxial phase and second from a biaxial phase to bent-director nematic phase with decrease in temperature. Every system was studied by changing the anchoring strength of the substrates and also in these cases it was observed that for the systems with lower anchoring strength, the specific heat did not give a signature of the ordering transition.

It is to noticed that the transition temperature increased with increase in the size of the system.

CONCLUSIONS

We have performed Monte Carlo simulations of a nematic film with hybrid boundary conditions. Our simulations are based on the

simplest successful lattice potential put forward to describe nematic liquid crystals (Lebwohl-Lasher). We have employed a standard Metropolis and a non-Boltzmann Monte Carlo methods. This latter and powerful method confirmed the assertion made by the work done using canonical Monte Carlo method and the mean field methods.

There are two transitions occurring in a hybrid nematic film with the change in temperature. With the decrease in temperature the first transition occurs at a temperature higher that the nematic isotropic transition, from a disordered phase to a biaxial nematic phase. The second occurs at a temperature lower than the nematic isotropic temperature, from a biaxial nematic phase to a bent-director nematic phase. The signatures of transitions were seen in the fluctuations in energy. The layer-wise order parameter and the layer-wise tilt angle with variation in temperature gave a clear indication of the different structures formed in a hybrid film with changes in temperature.

The transition became sharper with the increase in size of the liquid crystal film but there was also an increase in the transition temperatures. It is observed that the biaxiality present at the lower temperature (with bent structure) depends on the anchoring strength of the substrates and is fairly independent of the size of the system (Fig. 8). With the increase in the anchoring strength the biaxiality increases (Fig. 9). It is seen that a distortion develops in the bent-director with the reducing of the anchoring strength of the

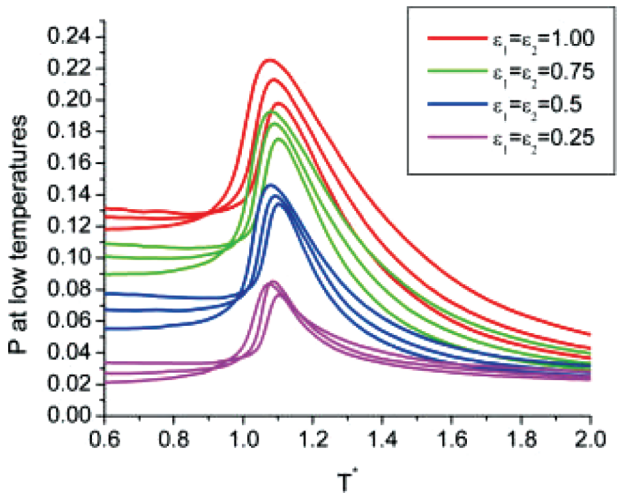

FIGURE 8 The biaxiality at lower temperatures with reduced temperature.

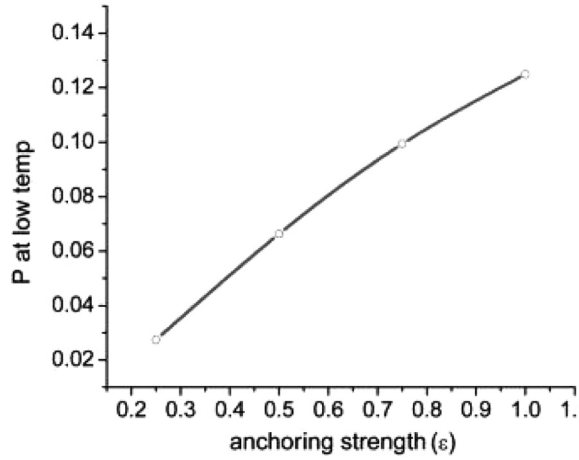

FIGURE 9 The variation of biaxiality with anchoring strength at low temperatures.

system (Fig. 10). The fluctuations in the tilt angle gave a deeper insight into the higher temperature transition which had no signature in the specific heat. The transition temperature increased with the size of the system (Fig. 11). The modified Wang-Landau Monte Carlo approach has proved to be very useful in the present work allowing the simulation of a greater number of state points, a high resolution in temperature, and, moreover, the easy determination of the free energy of the systems.

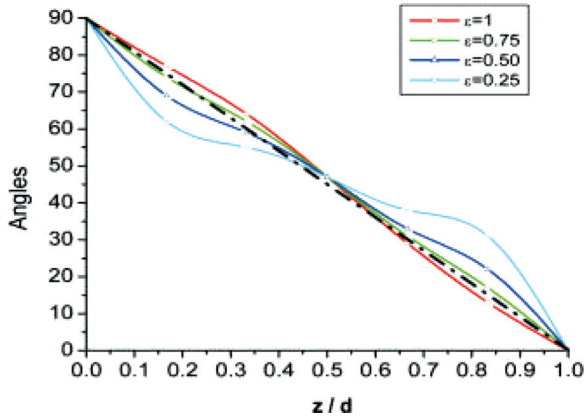

FIGURE 10 The bent director gets distorted with the decrease in the anchoring strength of the substrates simultaneously.

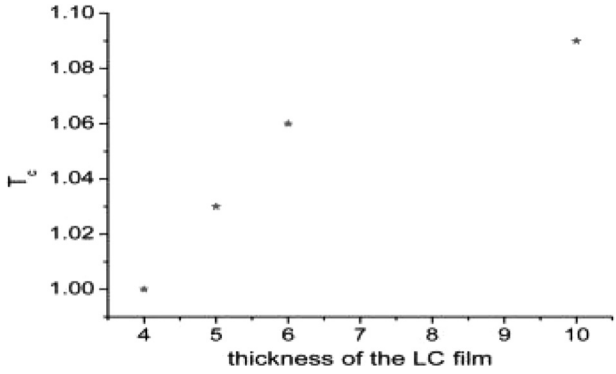

FIGURE 11 The variation of transition temperature with the liquid crystal film thickness (d).

REFERENCES

[1] Crawford, G. P. & Zumer, S., eds., (1996). *Liquid Crystals in Complex Geometries*, Taylor & Francis: London, *and references therein*.
[2] Rasing, T. & Musevic, I., eds., (2004). *Surfaces and Interfaces of Liquid Crystals*, Springer Verlag: Berlin.
[3] Pasini, P., Chiccoli, C., & Zannoni, C. (2000). Liquid crystal lattice models II. Confined systems. In: *Advances in the Computer Simulations of Liquid Crystals*, Pasini, P. & Zannoni, C. (Eds.), Kluwer: Dordrecht, 121.
[4] Zakharov, A. V. & Iwamoto, M. (2003). *J. Chem. Phys.*, *118*, 10758
[5] Chiccoli, C., Lavrentovich, O. D., Pasini, P., & Zannoni, C. (1997). *Phys. Rev. Lett.*, *79*, 4401.
[6] Chiccoli, C., Pasini, P., & Zannoni, C. (1999). *Mol. Cryst. Liq. Cryst.*, *336*, 123.
[7] Palffy-Muhoray, P., Gartland, E. C., & Kelly. (1994). *Liq. Cryst.*, *16*, 713.
[8] Sarlah, A. & Zumer, S. (1999). *Phys. Rev. E*, *60*, 1821.
[9] Cleaver, D. J. & Texeira, P. I. C. (2001). *Chem. Phys. Lett.*, *338*, 1.
[10] Chiccoli, C., Pasini, P., Sarlah, A., Zannoni, C., & Zumer, S. (2003). *Phys. Rev. E*, *67*, 050703.
[11] Sarlah, A. & Zumer, S. (2004). Introduction to micro- and macroscopic descriptions of nematic liquid crystalline films: Structural and fluctuation forces. In: *Surfaces and Interfaces of Liquid Crystals*, Rasing, T. & Musevic, I. (Eds.), Springer: Berlin 211.
[12] Lebwohl, P. A. & Lasher, G. (1972). *Phys. Rev. A*, *6*, 426.
[13] (a) Fabbri, U. & Zannoni, C. (1986). *Molec. Phys.*, *58*, 763; (b) Zhang, Z., Zuckermann, M. J. & Mouritsen, O. G. (1991). *Phys. Rev. Lett.*, *69*, 2803.
[14] Biscarini, F., Chiccoli, C., Pasini, P., Semeria, F., & Zannoni, C. (1995). *Phys. Rev. Lett.*, *75*, 1803.
[15] Chiccoli, C., Feruli, I., Lavrentovich, O. D., Pasini, P., Shyianovskii, S., & Zannoni, C. (2002). *Phys. Rev. E (R)*, *66*, 030701.
[16] Metropolis, N., Rosenbluth, A. W., Rosenbluth, M. N., Teller, A. H., & Teller, E. (1953). *J. Chem. Phys.*, *21*, 1087.
[17] Wang, F. G. & Landau, D. P. (2001). *Phys. Rev. Lett.*, *86*, 2050.
[18] Jayasri, D., Sastry, V. S. S., & Murthy, K. P. N. (2005). *Phys. Rev. E*, *72*, 036702.